doi: 10.15407/ujpe61.11.0980

V.V. VOITOVYCH,[1] R.M. RUDENKO,[1] V.O. YUCHYMCHUK,[2] M.V. VOITOVYCH,[2] M.M. KRASKO,[1] A.G. KOLOSIUK,[1] V.YU. POVARCHUK,[1] I.M. KHACHEVICH,[2] M.P. RUDENKO[3]

[1] Institute of Physics, Nat. Acad. of Sci. of Ukraine
(46, Nauky Prosp., Kyiv 03680, Ukraine; e-mail: vvoitovych@yahoo.com)
[2] V.E. Lashkaryov Institute of Semiconductor Physics, Nat. Acad. of Sci. of Ukraine
(45, Nauky Prosp., Kyiv 03028, Ukraine)
[3] Mykola Gogol State University of Nizhyn
(2, Krapyv'yanska Str., Nizhyn 16600, Ukraine)

PACS 68.55.Ln, 68.55.Nq

EFFECT OF TIN ON STRUCTURAL TRANSFORMATIONS IN THE THIN-FILM SILICON SUBOXIDE MATRIX

The processes of crystallization of amorphous silicon (a-Si) in the a-SiO_xSn ($1 \le x \le 2$) suboxide matrix have been studied. The temperature, at which the crystallization begins, is shown to be lower for a-SiO_xSn films with higher tin contents. For specimens with the maximum tin content (about 2 vol.%), the crystallization begins at a temperature of 500 °C; for specimens with the average tin content (about 1 vol.%), the crystallization temperature equals 800 °C; and for specimens with the minimum tin content (about 0.5 vol.%), the crystallization of a-Si starts at 1000 °C. On the other hand, it is shown that tin does not influence the separation of a-Si and the SiO_2 phase in the examined specimens. It is found theoretically that silicon crystallites that are formed during the crystallization of a-Si are much smaller ($d \approx 5 \div 7$ nm) in a-SiO_xSn films with a high tin content (1 and 2 vol.%) in comparison with the tin-free specimens ($d \ge 10$ nm). A metal-induced mechanism of crystallization of a-Si has been proposed, which predicts the existence of tin metal clusters in SiO_x that create conditions for the easier transition of the amorphous silicon phase into the crystalline one. On the basis of experimental data, it is supposed that, in our case, a necessary condition for the crystallization of a-Si by the proposed metal-induced mechanism to start is the presence of metal (tin) aggregates in SiO_x.

Keywords: crystallization, amorphous silicon, tin, nano-sized silicon crystallites.

1. Introduction

The ability of nanocrystalline silicon (nc-Si) in an amorphous SiO_2 matrix to emit visible light opens prospects for the creation of light-emitting elements that are compatible with the silicon technology [1]. Nowadays, the maximum quantum efficiency of light-emitting diodes on the basis of silicon oxide is equal to about 0.1% [2], whereas the commercially acceptable level amounts to about 10% [3]. The quantum efficiency of light-emitting elements on the basis of the nanocomposite material (nc-Si/SiO_2) is known to be determined by their radiation capacity. The latter, in turn, substantially depends on the nc-Si dimensions and the concentration in SiO_2.

© V.V. VOITOVYCH, R.M. RUDENKO, V.O. YUCHYMCHUK, M.V. VOITOVYCH, M.M. KRASKO, A.G. KOLOSIUK, V.YU. POVARCHUK, I.M. KHACHEVICH, M.P. RUDENKO, 2016

It is well known that the nc-Si/SiO_2 composite is created owing to the decay of the non-stoichiometric phase of silicon oxide (SiO_x, $0 < x < 2$) at elevated temperatures. This process can be schematically described by the reaction

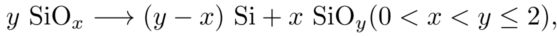

$$y\ SiO_x \longrightarrow (y - x)\ Si + x\ SiO_y (0 < x < y \leq 2),$$

where x is the initial index of the film stoichiometry, and y is its final value, which depends on the annealing temperature [4–7]. As a rule, silicon that emerges as a result of the transformation of SiO_x into SiO_2 is amorphous (a-Si) and begins to crystallize only at temperatures above 1000 °C.

As was shown in our previous works [8–11], the tin (Sn) metal impurity can substantially affect the crystallization of a-Si, as well as the concentration and dimensions of nc-Si in the amorphous SiO_2 matrix. In this work, the structural transformations and the processes of formation of nc-Si in thin films of silicon suboxide with various tin contents are studied.

2. Experimental Part

For our research, we fabricated four specimen batches of thin-film non-stoichiometric silicon oxide (a-SiO_xSn, $x \approx 1.2$) with various tin contents (see Table). The specimens were obtained by thermally evaporating the melted mixture of a SiO powder (Cerac Inc., a purity of 99.9%, a grain size of 40–45 μm) and a Sn powder of the PO-1 grade (a purity of 99.1%, a grain size of 40–45 μm) taken in various volume ratios (see Table). The evaporation was performed from a tantalum trunk in vacuum (about 10^{-3} Pa). The tantalum trunk was resistively heated up. Films were deposited onto silicon, quartz, and sapphire substrates. The substrate temperature at the deposition was equal to 300 °C. The film deposition rate was about 50 Å/s. In order to stimulate the transformation of the amorphous silicon oxide films into the amorphous-crystalline ones, the specimens were subjected to an isochronous thermal treatment (annealing) in a temperature interval of 300–1000 °C with a step of 100 °C in the argon atmosphere. The time of the annealing at each temperature amounted to 20 min. The thickness of the obtained films varied within the limits from 600 to 800 nm.

The structural researches were carried out, by using the Raman and infra-red (IR) spectroscopy. Raman spectra were registered at room temperature on a spectrometer T-64000 (Jobin Yvon). The spectra were excited, by using the radiation of an Ar laser with a wavelength of 514.5 nm. IR transmission spectra of a-SiO_x and a-SiO_xSn films were registered with the help of a Fourier spectrometer Spectrum BXII Perkin Elmer in the interval of antisymmetric Si–O–Si valence vibrations. The spectral measurements were carried out at room temperature with a resolution of 4 cm^{-1}.

3. Results and Their Discussion

Figure 1 demonstrates Raman spectra obtained for the thin-film specimens of all four batches (Table). The films were formed on sapphire substrates and isochronously annealed in the argon atmosphere. One can see that the amorphous phase is inherent to the as-sputtered specimens in all four batches, which is evidenced by a wide band with a maximum located at about 480 cm^{-1} [12]. In the specimens that belong to batches I and II and were thermally treated in a temperature interval from 300 to 900 °C, their structure remained amorphous up to a temperature of 900 °C inclusive. After the films had been annealed at 1000 °C, there emerged a phase of nanocrystalline silicon; this is evidenced by the appearance of a narrow band with a maximum at about 520 cm^{-1} in the Raman spectra [13–15]. At the same time, the crystalline phase nc-Si was formed already at a temperature of 800 °C in the specimens of batch III and at a much lower temperature of 500 °C in specimens of batch IV (see the bands in the corresponding Raman spectra at frequencies of about 516 and 517 cm^{-1}, respectively).

The Raman spectra of examined specimens were analyzed in the framework of the known "spatial phonon correlation" model [13]. The volume ratio f_{nc} between the crystalline phase of silicon and a-Si (see Fig. 2) and the average size of crystallites d

Parameters of mixtures for the sputtering of films

Specimen batch	Volume ratio between SiO_x and Sn powders
I: a-SiO_x	100 : 0
II: a-SiO_xSn1	100 : 0.5
III: a-SiO_xSn2	100 : 1
IV: a-SiO_xSn3	100 : 2

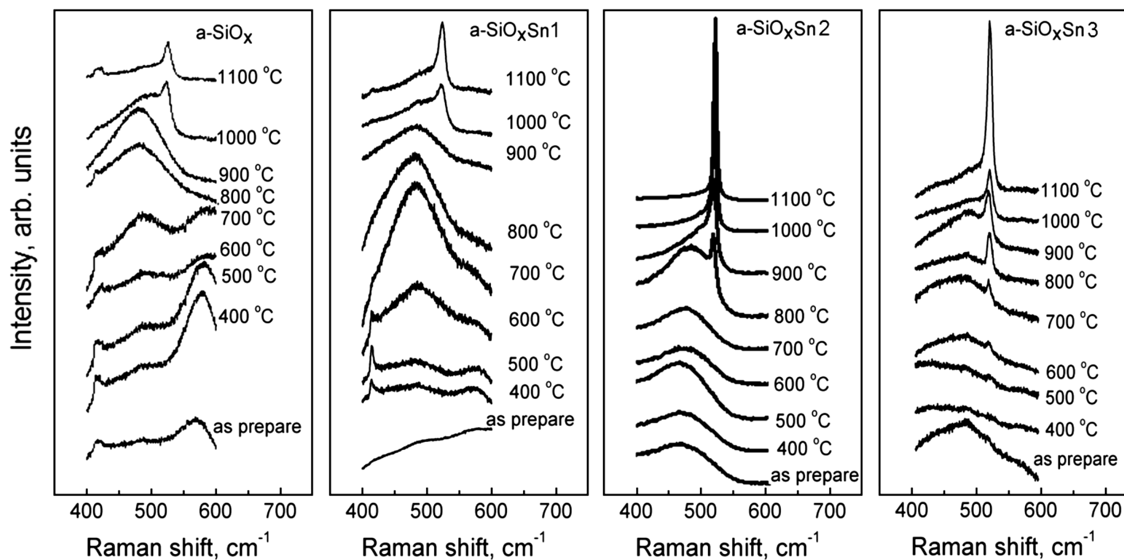

Fig. 1. Raman spectra for the specimens of batches I to IV measured immediately after the deposition on sapphire substrates and after subsequent isochronous annealing stages

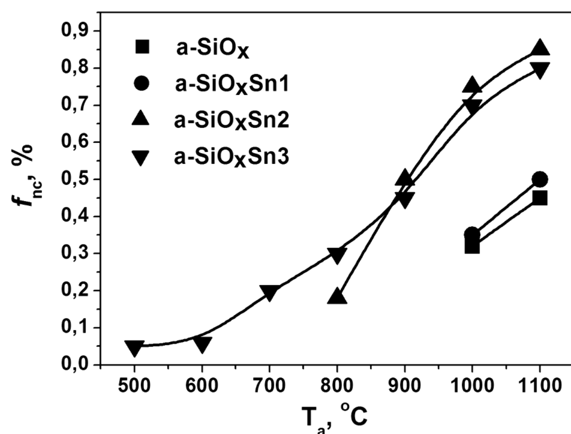

Fig. 2. Dependences of the volume fraction of the crystalline phase, f_{nc}, on the annealing temperature for the specimens of batches I–IV

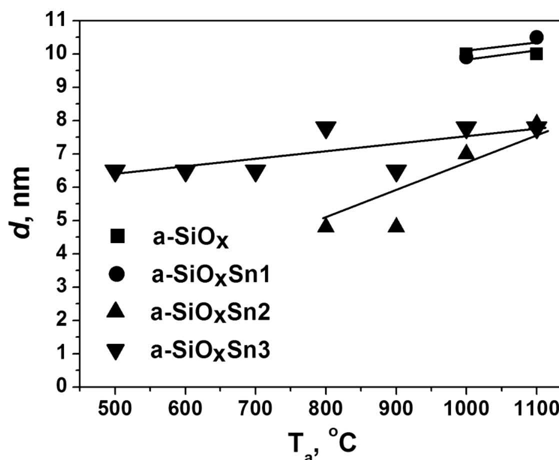

Fig. 3. Dependences of the average size of crystallites, d, on the annealing temperature for the specimens of batches I–IV

(see Fig. 3) were calculated. A procedure used for the determination of the ratio between the amorphous and crystalline phases of silicon, the dimensions and the concentration of silicon nanocrystals, and their dependences on the annealing temperature was described in our previous works [8, 11] in detail.

It is known that IR spectroscopy in the interval of Si–O–Si valence vibrations (600–1400 cm^{-1}) makes it possible to characterize the structural state of the SiO_y matrix and its transformation during the thermal annealing [16]. The authors of works [17, 18] experimentally established a relation between the nonstoichiometric value of y in SiO_y and the maximum position ν_{max} in the band associated with the IR absorption at Si–O–Si bonds. This relation is described well by the formula

$$y = 1+a(\nu_{\max}-980)+b(\nu_{\max}-980)^2-c(\nu_{\max}-980)^3, \quad (1)$$

where $a = 2.1\times10^{-3}$, $b = 1.05\times10^{-4}$, $c = 2.85\times10^{-7}$, and $\nu_{\max}$ is expressed in cm^{-1} units.

The IR absorption spectra of researched specimens in an interval from 700 to 1400 cm^{-1} were registered after every step of the isochronous thermal treatment in a wide temperature interval of 300–1100 °C. After each next step of the thermal treatment, a high-frequency shift of the aforementioned IR band from 1015 to 1107 cm^{-1} was observed, which testifies to the processes of phase separation into stoichiometric silicon oxide and nano-sized silicon [19–23]. As an example, Fig. 4 demonstrates the IR absorption spectra that were registered right after the specimen deposition (at 300 °C) and after the last step of the thermal treatment (at 1100 °C).

The visual analysis of the IR absorption spectra obtained for the specimens in all (I–IV) batches testifies that the tin impurity in oxide silicon films does not change the shape of those spectra and, accordingly, does not affect the processes of thermally induced phase separation. Using formula (1) and the positions $\nu_{\max}$ of the maximum in the IR absorption band experimentally measured for the researched specimens of batches I–IV, the dependence of the parameter y characterizing the non-stoichiometry of the SiO_y matrix on the annealing temperature was revealed (Fig. 5).

The volume ratio between the sum of the amorphous and nanocrystalline silicon components, V_{Si}, and silicon oxide emerging owing to the thermally induced phase separation can be calculated using the following formulas [19]:

$$V_{Si} = 1 - V_{SiO_y} = \frac{(y-1)M_{Si}\,\rho_{SiO_y}}{(y-1)\,M_{Si}\,\rho_{SiO_y} + M_{Si}\,\rho_{SiO_y}},$$
$$\rho_{SiO_y} = \frac{M_{SiO_y}\,\rho_{Si}\,\rho_{SiO}}{y\,M_{SiO}\,\rho_{Si} - (y-1)\,M_{Si}\,\rho_{SiO}}, \qquad (2)$$
$$\rho_{SiO} = \frac{2\,M_{SiO}\,\rho_{Si}\,\rho_{SiO_2}}{M_{SiO_2}\,\rho_{Si} + M_{Si}\,\rho_{SiO_2}},$$

where ρ_{Si}, ρ_{SiO_y}, ρ_{SiO}, and ρ_{SiO_2} are the densities of corresponding substances expressed in g/cm^3 units; M_{Si} = 28.09 g and M_{SiO_y} = 28.09 + 16x (in gram units) are the masses of gram-molecules of Si and SiO_y, respectively; and V_{SiO_y} is the volume fraction of the SiO_y matrix.

In Fig. 6, the dependence of V_{Si} on T_{ann} calculated according to formula (2) with the parameters ρ_{Si} = = 2.33 g/cm^{-3} and ρ_{SiO} = 2.18 g/cm^{-3}, and taking the experimental data from Fig. 5 into account is depicted. From this figure, it follows that, for all researched batches of specimens, the maximum value

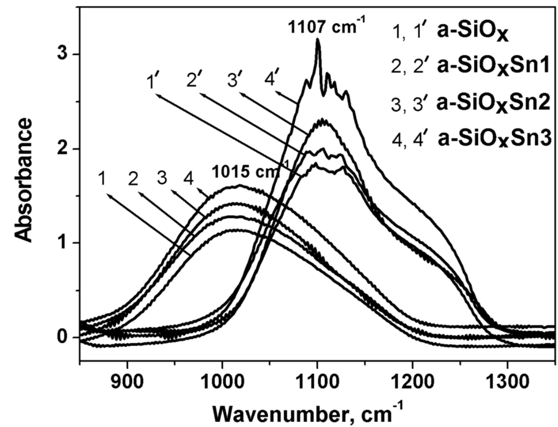

Fig. 4. IR absorption spectra of researched specimens: (*1* to *4*) as-fabricated specimens and (*1′* to *4′*) right after their thermal treatment at a temperature of 1100 °C

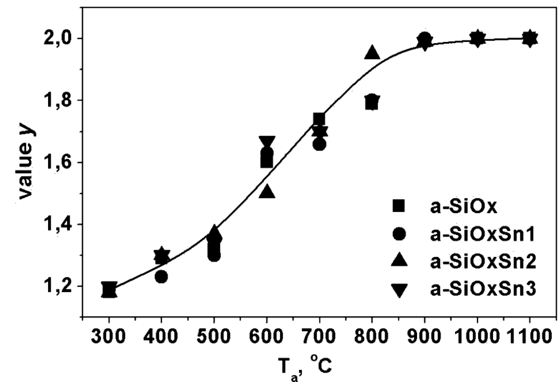

Fig. 5. Dependence of the non-stoichiometry parameter y for the SiO_y matrix of researched specimens on the annealing temperature

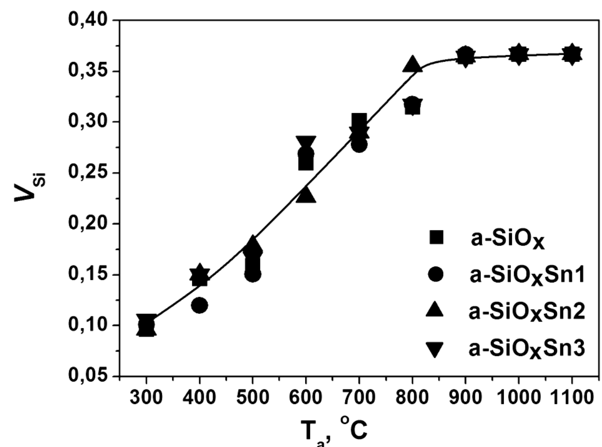

Fig. 6. Dependence of the total volume fraction of amorphous and nanocrystalline silicons, V_{Si}, on the annealing temperature

of $V_{\rm Si}$ ($\approx$0.36, i.e. about 36% of SiO_2) was reached at $T_{\rm ann} > 900$ °C.

From Fig. 6, one can also see that, at the annealing temperature $T_{\rm ann} \approx 500$ °C, the silicon volume fraction reached the value $V_{\rm Si} \approx 0.16$ in all batches of researched specimens. According to the data of works [24, 25], this value is the percolation threshold. When the volume fraction of silicon in nanoclusters exceeds the threshold value, the coalescence begins; namely, with a probability close to unity, some of isolated Si nanoclusters "stick to one another" to form Si nanothreads, which penetrate through the whole thickness of the SiO_y dielectric matrix.

On the basis of our results, we may assume that the mechanism of tin effect on the crystallization of amorphous silicon in the silicon oxide matrix can be similar to the mechanism of metal-induced crystallization. The latter, as is known, occurs when a-Si interacts with a metal droplet. As a rule, it occurs at the metal melting temperatures, and amorphous silicon dissolves in a liquid metal. At the same time, at temperatures below the metal melting point, the phase separation into crystalline silicon and the metal impurity in the solid state takes place [26–29]. Therefore, it is probable that the crystallization of a-Si in SiO_xSn specimens linearly depends on the concentration and the size of tin inclusions in the oxide matrix.

If the SiO_x matrix is doped with tin, some tin fraction, which does not exceed the solubility limit, dissolves in the oxide matrix, whereas the other fraction assembles into metal clusters. The latter govern, in what follows, the processes of amorphous silicon crystallization and the size of nanocrystals. The higher the tin content in a specimen, the higher the probability for the amorphous silicon phase to interact with metal inclusions. The probability of this interaction also increases during the coalescence of amorphous silicon nanoclusters. For example, the crystallization begins at a temperature of 500 °C in the specimens of batch IV ($V_{\rm Si} \approx 0.16$). This is the temperature, at which the coalescence of nanoclusters in amorphous silicon takes place. In the specimens of batch III–here, the tin content is lower–the crystallization begins at a higher temperature of 800 °C, at which $V_{\rm Si} \approx 0.3$. The corresponding sizes of silicon crystallites are slightly smaller than in the specimens of batch IV. In the specimens of batch II, the tin concentration most likely does not exceed the threshold of solubility in the SiO_x matrix. Therefore, the process of crystallization of a-Si in the specimens of batch II occurs at the same temperatures as in the tin-free specimens of batch I.

4. Conclusions

In this work, it is shown that the tin impurity in SiO_x films with $x \approx 1.2$ does not affect the transformation of SiO_x into SiO_2, but considerably reduces the temperature, at which the crystallization of amorphous silicon begins in the examined specimens. In addition, a decrease of the crystallization temperature correlates with a growth of the metal impurity content in the researched specimens. The crystallization begins at a temperature of 1000 °C in the specimens with the minimum tin content, at a temperature of 800 °C in the specimens with the medium tin content, and at 500 °C in the specimens with the maximum tin content. Moreover, a high tin content in the specimens of batches III and IV results in a reduction of the crystallite dimensions to about 5–7 nm. This value is considerably smaller than the size of crystallites ($\geq$10 nm) in the specimens with the minimum tin content (batch II) and in the tin-free specimens (batch I). On the basis of the obtained experimental results, the presence of metal aggregates of tin in SiO_x can be considered as a necessary condition for the crystallization of a-Si to start. In addition, the obtained data testify to the metal-induced mechanism of crystallization.

1. L.T. Canham. Silicon quantum wire array fabrication by electrochemical and chemical dissolution of wafers. *Appl. Phys. Lett.* **57**(10), 1046 (1990) [DOI: 10.1063/1.103561].
2. G. Franzo, A. Irrera, E.C. Moreira, M. Miritello, F. Iacona, D. Sanfilippo, G. Di Stefano, P.G. Fallica, F. Priolo. Electroluminescence of silicon nanocrystals in MOS structures. *Appl. Phys. A* **74**, 1 (2002) [DOI: 10.1007/s003390101019].
3. M.E. Castagna, S. Coffa, M. Monaco, L. Caristia, A. Messina, R. Mangano, C. Bongiorno. Si-based materials and devices for light emission in silicon. *Physica E* **16**, 547 (2003) [DOI: 10.1016/S1386-9477(02)00644-6].
4. I.P. Lisovskyy, I.Z. Indutnyy, V.G. Litovchenko, B.M. Gnennyy, P.M. Lytvyn, D.O. Mazunov, O.S. Oberemok, N.V. Sopinskyy, P.E. Shepeliavyi. Thermostimulated structural transformations in vacuum-evaporated SiO_x films. *Ukr. J. Phys.* **48**(3), 250 (2003).

5. A. Szekeres, T. Nikolova, A. Paneva *et al.* Silicon nanoparticles in thermally annealed thin silicon monoxide films. *Mater. Sci. Eng. B* **124–125**, 504 (2005) [DOI: 10.1016/j.mseb.2005.08.124].
6. S. Hayashi, T. Nagareda, Y. Kanazawa, K. Yamamoto. Photoluminescence of Si-rich SiO_2 films: Si clusters as luminescent centers. *Jpn. J. Appl. Phys.* **32**, 3840 (1993) [DOI: 10.1143/JJAP.32.3840].
7. M. Zacharias, J. Heitmann, R. Scholz *et al.* Size–controlled highly luminescent silicon nanocrystals: A SiO/SiO_2 superlattice approach. Appl. Phys. Lett. **80**, 661 (2002) [DOI: 10.1063/1.1433906].
8. V.V. Voitovich, V.B. Neimash, N.N.Krasko *et al.* Influence of Sn impurity on optical and structural properties of thin silicon films. *Fiz. Tekh. Poluprovodn.* **45**, 1331 (2011).
9. R.M. Rudenko, V.V. Voitovych, N.N. Krasko *et al.* Influence of high-temperature annealing on the structure and the intrinsic absorption edge of thin-film silicon doped with tin. *Ukr. Fiz. Zh.* **58**, 770 (2013).
10. R.M. Rudenko, M.M. Krasko, V.V. Voitovych *et al.* Behavior of hydrogen during crystallization of thin silicon films doped with tin. *Ukr. Fiz. Zh.* **58**, 1166 (2013).
11. V.V. Voitovich, R.N. Rudenko, A.G. Kolosyuk *et al.* Influence of tin on the processes of silicon nano-crystal formation in thin films of amorphous matrix SiO_x. *Fiz. Tekh. Poluprovodn.* **48**, 77 (2014).
12. A.A. Sirenko, J.R. Fox, L.A. Akimov, X.X. Xi, S. Ruvimov, Z. Liliental-Weber. In situ Raman scattering studies of the amorphous and crystalline Si nanoparticles. *Solid State Commun.* **113**, 553 (2000) [DOI: 10.1016/S0038-1098(99)00539-6].
13. H. Richter, Z.P. Wang, L. Ley. The one phonon Raman spectrum in microcrystalline silicon. *Solid State Commun.* **39**, 625 (1981) [DOI: 10.1016/0038-1098(81)90337-9].
14. H. Campbell, P.M. Fauchet. The effects of microcrystal size and shape on the one phonon Raman spectra of crystalline semiconductors. *Solid State Commun.* **58**(10), 739 (1986) [DOI: 10.1016/0038-1098(86)90513-2].
15. P. Mishra, K.P. Jain. First- and second-order Raman scattering in nanocrystalline silicon. *Phys. Rev. B* **64**, 073304 (2001) [DOI: 10.1103/PhysRevB.64.073304].
16. I.P. Lisovskyy, M.V. Voitovich, A.V. Sarikov, V.G. Litovchenko, A.B. Romanyuk, V.P. Melnyk, I.M. Khatsevich, P.E. Shepeliavyi. Transformation of the structure of silicon oxide during the formation of Si nanoinclusions under thermal annealings. *Ukr. Fiz. Zh.* **54**, 383 (2009).
17. M. Nakamura, Y. Mochizuki, K. Usami, Y. Itoch, T. Nozaki. Infrared absorption spectra and composition of evaporated silicon oxides (SiO_x). *Solid State Commun.* **50**(12), 1079 (1984) [DOI: 10.1016/0038-1098(84)90292-8].
18. V.N. Seminogov, V.I. Sokolov, V.N. Glebov *et al.* Percolation analysis of structural transformations and the formation of silicon nanoclusters at thermal annealing of SiO_x films. *Perspekt. Mater.* **8**, 159 (2010).
19. A.L. Shabalov, M.S. Feldman, M.Z. Bashirov. Vibrational spectra and structure of thin SiO_x films. *Izv. Akad. Nauk SSSR Ser. Fiz. Tekh. Mat. Nauk* **3**, 78 (1986).
20. A.P. Kucherov, S.M. Kochubei. Method for the resolition of a complicated contour into elementary components making use of the preliminary analysis of its structure. *Zh. Prikl. Spektrosk.* **38**, 145 (1983).
21. I.W. Boyd, J.I.B. Wilson. Silicon–silicon dioxide interface: An infrared study. *J. Appl. Phys.* **62**, 3195 (1987) [DOI: 10.1063/1.339320].
22. H.R. Philipp. Optical properties of non–crystalline Si, SiO, SiO_x and SiO_2. *J. Phys. Chem. Solids* **32**, 1935 (1971) [DOI: 10.1016/S0022-3697(71)80159-2].
23. I.P. Lisovskii. Dr. Sci. thesis *Structural Transformations in Near-Surface Layers of Silicon and Silicon-Oxygen Phases* (Kiev, 1998) (in Russian).
24. B.I. Shklovskii, A.L. Efros. *Electronic Properties of Doped Semiconductors* (Springer, 1984).
25. V.G. Golubev, V.Yu. Davydov, A.V. Medvedev, A.B. Pevtsov, N.A. Feoktistov. Raman scattering spectra and electric conductivity of thin silicon films with mixed amorphous–crystalline composition: determination of the volume fraction of nanocrystalline phase. *Fiz. Tverd. Tela* **39**, 1348 (1997).
26. O. Nast, S.R. Wenham. Elucidation of the layer exchange mechanism in the formation of polycrystalline silicon by aluminum-induced crystallization. *J. Appl. Phys.* **88**, 124 (2000) [DOI: 10.1063/1.373632].
27. A. Sarikov. Metal induced crystallization mechanism of the metal catalyzed growth of silicon wire-like crystals. *Appl. Phys. Lett.* **99**, 143102 (2011) [DOI: 10.1063/1.3644981].
28. O. Nast, T. Puzzer, L.M. Koschier. Aluminium-induced crystallization of amorphous silicon on glass substrates above and below the eutectic temperature. Appl. Phys. Lett. **73**, 3214 (1998) [DOI: 10.1063/1.122722].
29. V. Neimash, V. Poroshin, P. Shepeliavyi *et al.* Tin Induced a-Si Crystallization in Thin Films of Si-Sn Alloys. J. Appl. Phys. **114**, 213104 (2013) [DOI: 10.1063/1.4837661].

Received 10.12.15.
Translated from Ukrainian by O.I. Voitenko

В.В. Войтович, Р.М. Руденко, В.О. Юхимчук, М.В. Войтович, М.М. Красько, А.Г. Колосюк, В.Ю. Поварчук, І.М. Хацевич, М.П. Руденко

ВПЛИВ ОЛОВА НА СТРУКТУРНІ ПЕРЕТВОРЕННЯ ТОНКОПЛІВКОВОЇ СУБОКСИДНОЇ МАТРИЦІ КРЕМНІЮ

Р е з ю м е

Досліджено процеси кристалізації аморфного кремнію (a-Si) в субоксидній матриці a-SiO_xSn. Показано, що температура, при якій починається процес кристалізації, тим ниж-

ча, чим більше олова міститься в a-SiO_xSn плівках. Для зразків з максимумом олова (2% в об'ємі SiO_x) кристалізація починається при температурі 500 °C, для зразків з середнім значенням олова (1%) температура кристалізації становить 800 °C і для зразків з мінімумом олова (0,5%), процес кристалізації a-Si починається при 1000 °C. З іншого боку, показано, що олово не впливає на процеси розділення фаз a-Si та SiO_2 у досліджуваних зразках в процесі відпалу. З розрахунків встановлено, що у a-SiO_xSn плівках з високим вмістом олова (1 та 2%) в процесі кристалізації a-Si формуються кристаліти кремнію значно менших розмірів ($d \approx$ 5–7 нм) порівняно із нелегованими оловом зразками ($d \geq$ 10 нм). Запропоновано метало-індукований механізм кристалізації a-Si, який передбачає наявність металічних кластерів олова в SiO_x, які створюють умови для більш раннього переходу аморфної фази кремнію в кристалічну. Враховуючи експериментальні дані, ми припускаємо, що у нашому випадку необхідною умовою для початку кристалізації a-Si є наявність металічних скупчень олова в SiO_x, і має місце метало-індукований механізм кристалізації.